*Proceedings of the 15th International Conference on Industrial Engineering and Operations Management*
*Singapore, February 18-20, 2025*

*Proceedings of the International Conference on Industrial Engineering and Operations Management*

Publisher: IEOM Society International, USA DOI: 10.46254/AN15.20250523
Published: February 18, 2025

# Multimodal Resilience of an Engineered System Subject to Dependent Hazards

**Yian Wei**
PhD student, Department of Data and Systems Engineering
The University of Hong Kong
Pokfulam, Hong Kong
yianwei@connect.hku.hk

**Anchi Li**
PhD student, Department of Data and Systems Engineering
The University of Hong Kong
Pokfulam, Hong Kong
lianchi@connect.hku.hk

## Abstract

Many engineering systems face various natural and manmade hazards, whose occurrences can significantly disrupt system operations. The task of assessing how such systems perform under multiple hazards becomes especially challenging when hazards recur stochastically and influence one another in a dynamic manner. In this paper, we propose an analytical approach to model multiple dependent hazards, and use this model to quantify a system's multimodal performance (expressed as availability) and its resilience. Specifically, we derive the joint distribution for the hazards' occurrence and severity over time, then link that distribution to system degradation and recovery processes, ultimately determining the system's multimodal availability. By applying this method to the IEEE 9-bus modified test system as an approximation of the Western System Coordinating Council (WSCC) in the United States, we illustrate both the effectiveness and the practical relevance of our proposed approach to system performance evaluation.

## Keywords
Engineered systems, Dependent hazards, Availability, Resilience.

## 1. Introduction
Over the first two decades of the twenty-first century, large-scale critical systems have proliferated across numerous sectors. Any disruption or damage to these systems can have severe consequences for public health and a nation's economic stability. Besides the inherent failures a system may encounter—addressed through reliability analyses and preventive maintenance—external hazards, both natural and manmade, pose significant threats to overall functionality. Unlike inherent failures, these external hazards call for the use of resilience as an evaluation metric. Moreover, in many parts of the world, risks often involve multiple hazards simultaneously, amplifying the need for research into multi-hazard resilience.

In this paper, we model the multi-hazard resilience of an engineered system subject to recurrent hazards with interdependency. The three research objectives of this paper are listed as follows: characterization of the hazards that pose threats to system normal operation, modeling of system performance under the hazards, and quantification of system resilience based on the system performance.

## 2. Literature Review

To date, substantial studies have been conducted on topics that are related to the resilience modeling of an engineered system that is subject to multi hazards, including hazards characterization and system performance and resilience modeling under such multi hazards. A brief review is given below.

**Scenario-Based (Deterministic) and Probabilistic Hazard Characterization.** Many researchers have approached multi-hazard modeling by focusing on specific hazards within particular regions, often emphasizing scenario-based methods that rely on historical data and do not always incorporate explicit stochastic models for frequency and severity. For instance, Bangladesh—a nation extremely vulnerable to natural disasters—has district-level multi-hazard zoning ((Barua et al., 2016)), where consequences of each hazard type are derived from historical disaster records. Similar work by (Bathrellos et al., 2017) merges single-hazard maps (landslides, floods, earthquakes) into an integrated multi-hazard overview for Northeastern Peloponnesus, Greece. Another example is the assessment of landslide hazards on Madeira Island, which led to cascading hazards after a severe rainfall event in February 2010 ((Nguyen et al., 2013)). On the other hand, it is widely recognized that hazards exhibit randomness in both frequency and severity, making probabilistic methods crucial for robust mitigation planning. Popular probability distributions to capture hazard occurrence include Poisson (homogeneous or non-homogeneous) and Binomial processes, whereas severity can sometimes be modeled by distributions like the Binomial or other approaches. Researchers also categorize methods to account for such interactions as qualitative, semi-quantitative, or fully quantitative. Qualitative models ((Di Mauro et al., 2006) and (Marzocchi et al., 2012)) offer frameworks and guidelines without heavy numerical detail, while semi-quantitative methods use matrices and event trees ((Kong and Simonovic, 2019) and (Marzocchi et al., 2009)). Quantitative models, whether nonparametric (e.g., random forest, probability maps, Copula functions) or parametric (e.g., joint probability approaches, multiple regression, Bayesian networks), rigorously capture dependency structures among hazards.

**Deterministic and probabilistic Modeling of Performance or Resilience.** Building on multi-hazard characterizations, researchers often evaluate performance or resilience under specific hazards, frequently emphasizing localized settings. For example, (Preston et al., 2016) examines power grid resilience in the United States by scrutinizing the entire hazard spectrum. Arizona's flood-wildfire-drought mitigation plan likewise addresses multiple perils, though each hazard is mostly considered independently ((Srivastava and Laurian, 2006)). A number of probabilistic frameworks address the performance (or, in terms of reliability) modelling and optimization of a system (Li et al., 2024, Wei et al., 2024, Gao et al., 2021, Cheng et al., 2021b, Zhao et al., 2025, Wei et al., 2025) or a population of systems (Cheng et al., 2021c) that are subject to multiple sources of stresses or external shocks. Based on the modelling and optimization work, criticality analysis is conducted (Zou et al., 2023b, Wang et al., 2022, Zou et al., 2023a).

**Discussions.** Despite some progress in describing dependent multi-hazards (often drawing on historical or simulated data), existing frameworks remain fairly narrow in scope. They usually emphasize specific hazards in particular regions rather than covering the full range of possible hazardous events. Additionally, any interdependence among hazards—when accounted for—tends to be treated as a static parameter, such as through a hazard matrix. This assumption does not accurately represent realistic scenarios where hazards unfold and interact dynamically over time. Furthermore, hazards often occur multiple times, each with random timing and severity, making it complex to capture their interrelations fully. These considerations underscore the need for probabilistic models that depict random hazards—both in occurrence and severity—while incorporating evolving interdependencies over extended time horizons.

Although many studies examine performance under a variety of hazards, a common strategy is to treat each hazard independently, then combine the individual performance losses (e.g., via summation or averaging). Such methods do not address scenarios in which hazards arise in a random, interacting fashion that influences how they jointly compromise system functionality. While some dynamic studies exist, they are often simulation-based and do not explicitly handle hazards' repeated occurrences in an analytical manner. Consequently, there is a pressing need for a suitable system performance indicator along with an analytical framework that can capture how dependent, recurring hazards jointly shape overall system performance.

Extending the idea of multi-modal performance to a corresponding notion of resilience presents significant hurdles. Various resilience metrics have been proposed, including (i) measures of performance across a time window ((Cimellaro et al., 2010)), (ii) performance at particular time points ((Ouyang, 2017)), (iii) probability-based assessments of meeting robustness or recovery standards ((Giahi et al., 2020)), and (iv) integrative indicators across the entire hazard-recovery timeline ((Chang and Shinozuka, 2004)). However, these approaches tend to assume (a) an overall monotonic decline in system performance followed by a similarly monotonic recovery, or (b) a single hazard-recovery phase. They do not typically identify specific turning points in performance or address cases where multiple hazards occur sequentially (or overlapping) and induce repeated cycles of damage and recovery, leading to multi-modal performance trajectories. Indeed, in reality, hazards can recur over multiple intervals, creating multiple hazard-recovery cycles, as suggested by Figure 1. When performance falls or recovers in a non-linear or multi-phase manner, existing resilience metrics struggle to capture these dynamics. Hence, a more advanced approach is needed for multi-modal resilience quantification that reflects the discontinuous and repeated nature of real-world hazard events.

In this study, we focus on three core challenges. First, we propose a set of statistical models that capture the dynamic occurrence frequency and severity of multiple, dependent hazards with recurrence, where a hazard's occurrence probability and severity are both elevated by the presence of other relevant hazards within a specified time frame. We then derive the joint distribution for the occurrence times and severities of all hazards acting upon a given system. Next, we introduce a method to characterize multimodal availability, reflecting the varying performance levels of systems with multiple performance indicators—each one vulnerable to different hazards. Specifically, we describe how performance degrades and recovers under these interdependent, recurrent hazards, and we analytically track the system's overall performance over time. For our purposes, we consider availability to be the system's overarching performance metric. Finally, we formulate several multimodal resilience measures. A key element here is our segment division algorithm, which helps smooth out the system's multimodal availability profile and enables an efficient representation of the system's resilience over time. We further investigate the properties of instantaneous resilience, highlighting issues of convexity and monotonicity. To validate the precision, applicability, and effectiveness of our proposed models, we provide simulation results and numerical examples.

## 3. Hazards Characterization

We consider a system that is vulnerable to a set of hazards $\mathbf{\Omega}$. For an arbitrary hazard $i \in \mathbf{\Omega}$, its occurrence frequency is positively correlated with the occurrence and severity of its dependent hazard set $\mathbf{\Omega}_i^{fre}$. Similarly, the severity of hazard $i \in \mathbf{\Omega}$ upon each occurrence is positively correlated with the occurrence and severity of its dependent hazard set $\mathbf{\Omega}_i^{sev}$. In this section, we characterize the frequency and severity of hazard *i,* and model the joint distribution of the occurrence time and severity of all hazards in $\mathbf{\Omega}$ over time.

3.1 *Hazards Frequency and Severity*

***Frequency.*** The occurrence of hazard *i* follows a Non-homogenous Poisson process with a counting process $N_i(s) \sim P(\int_0^s \lambda_i(t)dt)$, where $\lambda_i(t)$ is the summation of (i) its inherent occurrence rate $\lambda_i^0(t)$ (which is independent of other hazards) and (ii) the impact of the occurrence time and severity of the hazards in $\mathbf{\Omega}_i^{fre}$ on its occurrence rate (Eq. (1)). Both (i) and (ii) are dynamic.

$$\lambda_i(t) = \lambda_i^0(t) + \sum_{j \in \Omega_i^{fre}} \sum_{\forall \beta: t_{j\beta} \in (t_{i\alpha} - \tau_{ji}^{fre}, t_{i\alpha})} \lambda_i(S_{j\beta}) \tag{1}$$

***Severity.*** Upon each occurrence, hazard *i*'s severity is modeled as the summation of (i) its inherent severity $S_i^0$ (which is independent of other hazards and randomly distributed with a CDF $F_i^0(\cdot)$) and (ii) the impact of the occurrence time and severity of the hazards in $\mathbf{\Omega}_i^{sev}$ (Eq. (2)). It is modelled by

$$S_{i\alpha} = S_i^0 + \sum_{\forall j \in \Omega_i^{Sev}} \sum_{\forall \beta: t_{j\beta} \in (t_{i\alpha} - \tau_{ji}^{sev}, t_{i\alpha})} S_{i\alpha}(S_{j\beta}) \tag{2}$$

3.2 *A Joint Distribution of the Hazards Occurrence Time and Severity*

We investigate the joint probability density function (pdf) of $\vec{T}_i$ and $\vec{S}_i$ $\forall i \in \mathbf{\Omega}$ in Eq. (3). Specifically, the joint pdf is obtained by exploring the conditional pdf of $\vec{T}_i$ and $\vec{S}_i$ given the frequencies and severity levels of all the hazards in $\Omega_i^{fre} \cup \Omega_i^{sev}$. Its explicit form is given by

$$P\left(\vec{T}_i = \vec{t}_i, \vec{S}_i = \vec{s}_i; \forall i \in \Omega\right) = \prod_{i \in \mathbf{\Omega}} P\left(\vec{S}_i = \vec{s}_i \middle| \vec{t}_i, \vec{t}_j, \vec{s}_j \forall j \in \Omega_i^{sev}\right) P\left(\vec{T}_i = \vec{t}_i \middle| \vec{t}_j, \vec{s}_j \forall j \in \Omega_i^{fre}\right) \tag{3}$$

where

$$P\left(\vec{S}_i = \vec{s}_i \middle| \vec{t}_i, \vec{t}_j, \vec{s}_j \forall j \in \Omega_i^{sev}\right) = \prod\nolimits_{\forall \alpha} \left(\left(f_i^0\left(s_{i\alpha}^0\right) * \prod\nolimits_{\forall j \in \Omega_i^{sev}, \forall \beta: t_{j\beta} \in (t_{i\alpha} - \tau_{j,i}^{sev}, t_{i\alpha})} * f_{ij}\left(s_{i\alpha}; s_{j\beta}\right)\right)[s_{i\alpha}]\right) \tag{4}$$

$$P\left(\vec{T}_i = \vec{t}_i \middle| \vec{t}_j, \vec{s}_j \forall j \in \Omega_i^{fre}\right) = \prod\nolimits_{\forall \alpha} \lambda_i\left(t_{i\alpha}\right) \exp\left(\sum\nolimits_{\forall \alpha}\left(-\int_{t_{i(\alpha-1)}}^{t_{i\alpha}} \lambda_i(\mu)\, d\mu\right)\right) \tag{5}$$

$$\lambda_i(\mu) = \lambda_i^0(\mu) + \sum\nolimits_{j \in \Omega_i^{fre}} \sum\nolimits_{\forall \beta: t_{j\beta} \in \vec{T}_j \,\&\, \mu - \tau_{j,i}^{fre} \le t_{j\beta} \le \mu} \lambda_i(S_{j\beta}).$$

When hazard *i*'s frequency and severity are independent of other hazards, i.e., $\Omega_i^{fre} \cup \Omega_i^{sev} = \varnothing$, Eq. (3) is reduced to Eq. (6):

$$P\left(\vec{T}_i = \vec{t}_i, \vec{S}_i = \vec{s}_i\right) = P\left(\vec{S}_i = \vec{s}_i \mid \vec{t}_i\right) P\left(\vec{T}_i = \vec{t}_i\right) = \prod\nolimits_{\forall \alpha} P(S_{i\alpha} = s_{i\alpha}) \left(\lambda_i^0(t_{i\alpha}) \exp\left(-\int_{t_{i(\alpha-1)}}^{t_{i\alpha}} \lambda_i^0(t) dt\right)\right) \tag{6}$$

# 4. Modeling of System Multimodal Availability

## 4.1 System Performance Degradation and Recovery Processes

We consider that the system has a set of independent performance indicators $\Theta$. Upon each occurrence of hazard *i*, system performance indicator *i* stochastically degrades for a fixed period $\tau_i$. Hazard *i* occurs repeatedly over time and the degradation level of performance indicator *i* accumulates. Upon system's failure, a recovery action starts to recover all degraded performance indicators to the pre-hazard levels. We define two system states (the system is in either state 1 or state 2 at an arbitrary time) and describe the system state transition process as follows.

*State* 1 (i.e., performance degradation process): The system is not under recovery and is available.
*State* 2 (i.e., performance recovery process): The system is under recovery and is unavailable.

State 1. At time $t = 0$, the system is in state 1. An arbitrary hazard *i* may occur at arbitrary time instants and stochastically degrade system performance indicator *i*. We develop a non-stationary Gamma process with a dynamic stepwise shape parameter $\alpha_i(t) = \sum\nolimits_{\forall \alpha: t - \tau_i < t_{i\alpha} \le t} S_{i\alpha}$ to model system performance indicator *i* degradation process over time (Eqs. (7) - (8)).

$$D_i(0) = D_i^0 \tag{7}$$

$$\lim_{\Delta t \to 0} D_i(t + \Delta t) = D_i(t) + G(\Delta t; \alpha_i(t), \beta_i), \quad t \in \left(0, t_1^2\right) \tag{8}$$

State 2. The recovery action starts at time $t_1^2$ to recover all degraded performance indicators to the corresponding pre-hazard levels. We develop a non-stationary Wiener process with a dynamic stepwise drift parameter $\gamma_i(t) = \gamma_i^0 - \sum\nolimits_{\forall \alpha: t - \tau_i \le t_{i\alpha} \le t} S_{i\alpha}$ to characterize the recovery process with respect to performance indicator *i* (Eq. (9)). The recovery action lasts until all degraded performance indicators are recovered, upon which the system transits back to state 1 at time $t_2^1$ (i.e., re-enters state 1 for the 2nd time).

$$\lim_{\Delta t \to 0} D_i(t + \Delta t) = \begin{cases} D_i(t) + \gamma_i(t)\Delta t + N(0, \sigma_i^2 \Delta t) & \text{if } D_i(t_1^2) > 0 \\ 0 & \text{if } D_i(t_1^2) = 0 \end{cases} \tag{9}$$

## 4.2 *System Multimodal Availability Modeling*

System availability at time *t* equals to the probability that it is in state 1. Its expression is given by

$$A(t)=\sum_{m=1}^{\infty}P\left(t_m^2>t\right)=\sum_{m=1}^{\infty}\int_{t_m^1=0}^{t}P\left(t_m^2>t\mid t_m^1\right)\cdot P\left(T_m^1=t_m^1\right)\cdot dt_m^1 \tag{10}$$

where

$$P\left(t_m^2>t\mid t_m^1\right)=\prod_{\forall i\in\mathbf{\Omega}}P(D_i(t-t_m^1)<D_i^F\mid t_m^1)=\prod_{\forall i\in\mathbf{\Omega}}F_G(D_i^F-D_i^0;\sum_{\forall\alpha:t_m^1-\tau_i\le t_{i\alpha}\le t}S_{i\alpha}\left(\min\left(\tau_i,t-t_{i\alpha},t_{i\alpha}+\tau_i-t_m^1\right)\right),\beta_i\ ) \tag{11}$$

$$P\left(T_m^1=t_m^1\right)=\prod_{\beta=1}^{m}\int_{t_\beta^1=t_{\beta-1}^1}^{t}P\left(T_{\beta+1}^1=t_{\beta+1}^1\middle|t_\beta^1\right)\cdot\prod_{\beta=1}^{m}dt_\beta^1 \tag{12}$$

We particularly investigate $P\left(T_{\beta+1}^1=t_{\beta+1}^1\middle|t_\beta^1\right)$ in Eq. (12) by exploring system's possible transitions between state 1 and state 2 as follows.

$$P\left(T_{\beta+1}^1=t_{\beta+1}^1\middle|t_\beta^1\right)=\sum_{i\in\mathbf{\Omega}}\sum_{i'\in\Omega}\int_{t_\beta^1}^{t_{\beta+1}^1}P_{i,i'}\left(T_{\beta+1}^1=t_{\beta+1}^1,T_\beta^2=t_\beta^2\middle|t_\beta^1\right)dt_\beta^2 \tag{13}$$

where

$$\begin{aligned}P_{i,i'}\left(T_{\beta+1}^1=t_{\beta+1}^1,T_\beta^2=t_\beta^2\middle|t_\beta^1\right)=P\left(D_i\left(t_\beta^2\right)=D_i^F\right)\cdot\prod_{\forall j\neq i\,\&\,j\in\Omega}\int_{D_j=0}^{D_j^F}P\left(D_j\left(t_\beta^2\right)=D_j\right)dD_j\\ P\left(\inf\left\{t\middle|D_{i'}(t_{\beta+1}^1)=D_{i'}^0;t>t_\beta^2\right\}=t_{\beta+1}^1\right)\cdot\prod_{\forall j'\neq i'\,\&\,j'\in\Omega}P\left(\inf\left\{t\middle|D_{j'}\left(t\right)=D_{j'}^0;t>t_\beta^2\right\}<t_{\beta+1}^1\right)\end{aligned} \tag{14}$$

It is worth noting that most real-world infrastructures that these proposed availability models target share two key features. First, they typically comprise multiple subsystems. Therefore, when evaluating the infrastructure's overall availability, it is necessary to identify how these subsystems connect or depend on one another, and then aggregate each subsystem's availability into a single measure for the entire infrastructure. Second, many infrastructures do not fall neatly into "failed" versus "operational" states but may instead have "partial functionality." In such circumstances, using "availability" alone may not accurately capture the infrastructure's actual performance. Consequently, other measures—such as the expected fraction of normal functions delivered—are more appropriate.

## 5. Case Study

Unanticipated disturbances leading to blackouts are a central concern for power grids. In this work, we illustrate our proposed availability and resilience approaches using the widely referenced IEEE 9-bus modified test system, which approximates the Western System Coordinating Council (WSCC) in the United States. This system includes nine buses, six connectors, three transformers, and three users. Given known load demands and generator statuses, power flow and bus voltages can be calculated via the Newton-Raphson method (whose detailed steps are standardized and thus not reproduced here). An important point is that, because the system incorporates redundancy—such as a slack generator and parallel transmission lines—it can typically maintain operation despite intrinsic failures (for example, short circuits or ground faults). Consequently, those inherent failures are not modeled in our analysis. Instead, the focus is on random natural and human-induced hazards, which can substantially disrupt power generation, transmission, and distribution. A graphic representation of the system is given below in Figure 1.

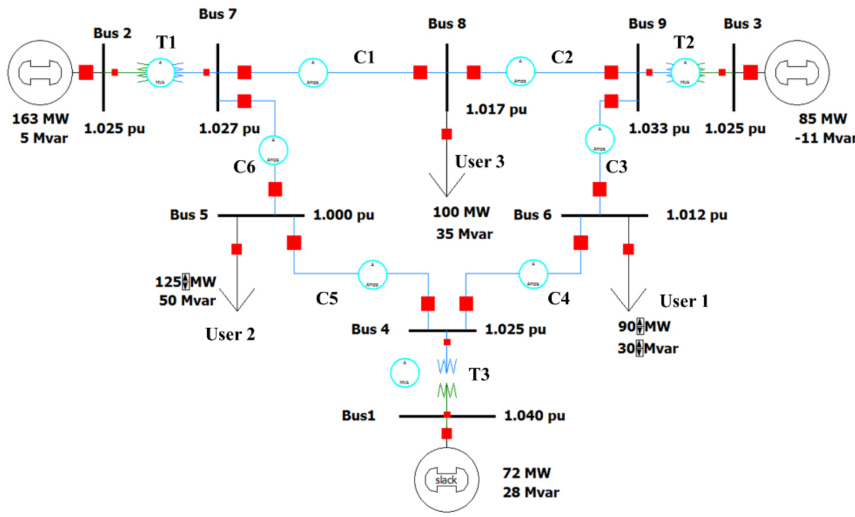


Figure 1. IEEE 9-bus modified test system

We consider three major hazards that pose the greatest risk to the IEEE 9-bus system's reliable performance.
**Cyber-Attack (Hazard 1)**. This hazard primarily targets the distribution control systems housed within the buses, where programmable logic controllers (PLCs) manage power distribution. It is further complicated by the reliance of distributed energy resources on open communication networks, making them susceptible to infiltration or data manipulation.
**Extreme Wind (Hazard 2).** High wind speeds can uproot trees, snap power lines, and disrupt service to distribution substations. All major components—buses, connectors, and transformers—are at risk from such powerful gusts, which can lead to outages or physical damage in the network.
**Wildfire (Hazard 3)**. Wildfire poses a serious threat to buses, connectors, and transformers. Moreover, its damaging effects become significantly greater when coupled with extreme wind, which can carry embers over larger distances and intensify the heat, thereby amplifying the overall impact.

Three distinct hazards are each modeled as Poisson processes for their occurrence, with severity drawn from normal distributions. Table 1 summarizes the base (or "inherent") frequency and severity parameters for all three. Dependencies exist specifically between wildfire and extreme wind, as shown in Table 2. In particular, the presence of extreme wind (i) raises the probability that a wildfire will occur, and (ii) heightens the wildfire's potential damage within a relevant time window. Meanwhile, the degradation and recovery behaviors for buses, transformers, and connectors under any of the three hazards follow Gamma processes (for performance decline) and Wiener processes (for repair), using the parameters presented in Table 3. These parameters include the Gamma scale factors, the intrinsic repair rates, the Wiener diffusion terms, and the critical failure thresholds for each type of component.

Table 1. Hazards' inherent frequency and severity

| $\lambda_1^0(t)$ | $\lambda_2^0(t)$ | $\lambda_3^0(t)$ | $f_1^0(\cdot)$ | $f_2^0(\cdot)$ | $f_3^0(\cdot)$ | $\tau_1$ | $\tau_2$ | $\tau_3$ |
|---|---|---|---|---|---|---|---|---|
| 0.01 | 0.007 | 0.001 | $N(1.2,0.1)$ | $N(1,0.1)$ | $N(1,0.1)$ | 50 | 50 | 50 |

•

Table 2. Dependency between extreme wind and wildfire

| $\tau_{23}^{fre}$ | $\tau_{23}^{sev}$ | $\lambda_3(S_2)$ | $f_{23}(\cdot;S_2)$ |
|---|---|---|---|
| 50 | 50 | $S_2/200$ | $S_2 \times N(0.5,0.1)$ |

Table 3. Degradation and recovery processes of the bus, transformer and connector under the hazards

| | $\beta_1$ | $\beta_2$ | $\beta_3$ | $\gamma_1$ | $\gamma_2$ | $\gamma_3$ | $\sigma_1^2$ | $\sigma_2^2$ | $\sigma_3^2$ | $D_1^F$ | $D_2^F$ | $D_3^F$ |
|---|---|---|---|---|---|---|---|---|---|---|---|---|
| Bus | 5 | 5 | 10 | 20 | 25 | 15 | 25 | 16 | 16 | 200 | 200 | 150 |
| Transformer | NA | 8 | 10 | NA | 25 | 15 | NA | | | NA | 200 | 150 |
| Connector | NA | 10 | 15 | NA | 40 | 25 | NA | | | NA | 150 | 100 |

Utilizing the models outlined in Section 3, we calculate the joint distribution of occurrence times and severities for the three hazards over the specified period. From these results, we determine the bus, transformer, and connector availabilities shown in Figure 2. Building on that, we compute the overall system performance—defined as the proportion of customers whose demand is satisfied—and plot it in Figure 3. Figure 4 reveal a similar monotonicity trend in the availabilities of the three component types (bus, transformer, connector) and in the overall system performance. Initially, all remain high because, at the outset, none of the hazards has occurred nor has any degradation crossed the failure thresholds for these components. This period of relative stability continues until increasing hazard occurrence probabilities begin to lower each component's availability. Observing the entire system's performance, we see that during the first half of the recovery window, it rises steadily, but then enters a phase of fluctuations as the recovery continues. In essence, as the probability of recurring hazards grows, it can slow down the expected recovery process for buses, transformers, and connectors. We refer to the segment division algorithm to smooth out the system performance curve. We then use the resilience metric in (Cheng et al., 2021a) to evaluate the system resilience, the weight of system performance is set to be dynamic as $w(t_n; t_{(x)} \le t_n \le t_{(x+1)}) = 1 - \sqrt{\dfrac{t_n}{t_{(x+1)} - t_{(x)}}}$.

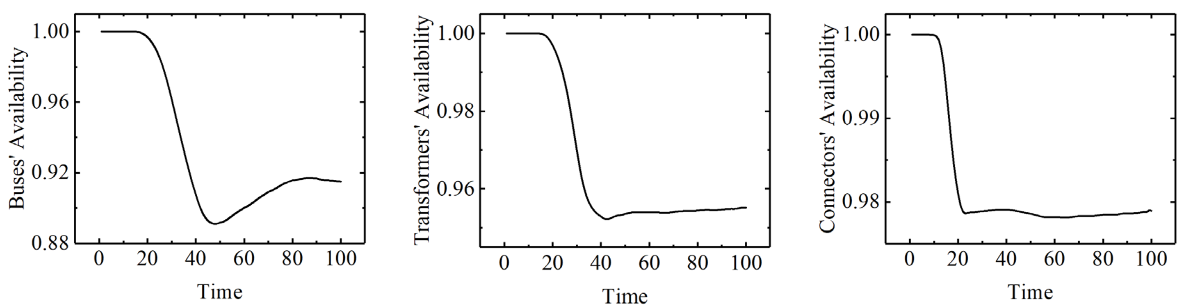


Figure 2. Availability of the components over period $(0,100)$

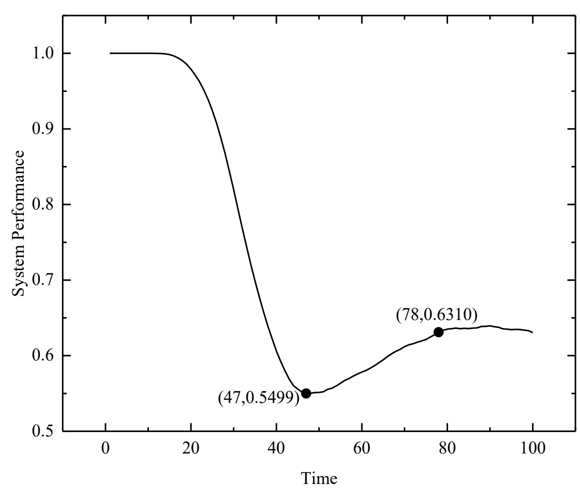


Figure 3. Performance of the IEEE 9-bus system over period $(0,100)$

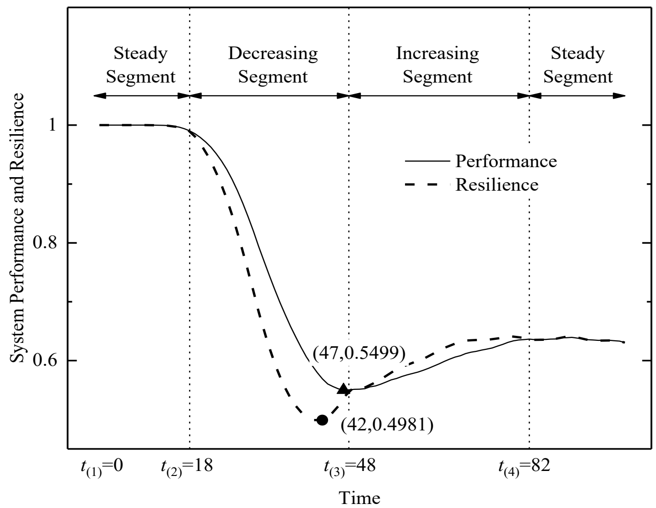


Figure 4. System performance and resilience over period (0,100)

We can see that as time progresses, under dependent hazards, hazards occur continuously due to their interdependency. Consequently, unlike a typical one-time hazard, neither resilience nor performance can return to their pre-disruption levels.

## 6. Conclusion

This paper presents an analytical framework for assessing both performance (interpreted here as availability) and resilience in systems subject to dependent, recurring random hazards. Our approach begins by providing a quantitative description of each hazard's occurrence frequency and severity, recognizing that one hazard can elevate another's likelihood (and impact) when they occur concurrently. We derive the joint distribution for hazard occurrence times and severities for all hazards relevant to the system. Building on this characterization, we then model how the system's performance degrades and recovers in the presence of these hazards, leading to a time-varying, multimodal depiction of system availability. We further define several resilience measures—namely, instantaneous, overall, and average resilience—that rely on availability to capture system performance, robustness, and recovery capabilities. The accuracy and practical utility of these proposed availability and resilience formulations are corroborated by both simulation and numerical case studies.

## References

Barua, U., Akhter, M. S. & Ansary, M. A. District-wise multi-hazard zoning of Bangladesh. *Natural Hazards,* 82**,** 1895-1918. 2016.

Bathrellos, G. D., Skilodimou, H. D., Chousianitis, K., Youssef, A. M. & Pradhan, B. Suitability estimation for urban development using multi-hazard assessment map. *Science of the total environment,* 575**,** 119-134. 2017.

Chang, S. E. & Shinozuka, M. Measuring improvements in the disaster resilience of communities. *Earthquake spectra,* 20**,** 739-755. 2004.

Cheng, Y., Elsayed, E. & Chen, X. Random Multi Hazard Resilience Modeling of Engineered Systems and Critical Infrastructure. *Reliability Engineering & System Safety***,** 107453. 2021a.

Cheng, Y., Elsayed, E. A. & Chen, X. Random Multi Hazard Resilience Modeling of Engineered Systems and Critical Infrastructure. *Reliability Engineering & System Safety,* 209. 2021b.

Cheng, Y., Liao, H. T. & Huang, Z. Y. Optimal Degradation-Based Hybrid Double-Stage Acceptance Sampling Plan for a Heterogeneous Product. *Reliability Engineering & System Safety,* 210. 2021c.

Cimellaro, G. P., Reinhorn, A. M. & Bruneau, M. Framework for analytical quantification of disaster resilience. *Engineering structures,* 32**,** 3639-3649. 2010.

Di Mauro, C., Bouchon, S., Carpignano, A., Golia, E. & Peressin, S. Definition of multi-risk maps at regional level as management tool: experience gained by civil protection authorities of Piemonte region. Proceedings of the 5th Conference on Risk Assessment and Management in the Civil and Industrial Settlements, 17-19. 2006.

Gao, Y., Wang, J. W., Gao, S. & Cheng, Y. An Integrated Robust Design and Robust Control Strategy Using the Genetic Algorithm. *IEEE Transactions on Industrial Informatics,* 17**,** 8378-8386. 2021.

Giahi, R., MacKenzie, C. A. & Hu, C. Design optimization for resilience for risk-averse firms. *Computers & Industrial Engineering,* 139. 2020.

Kong, J. & Simonovic, S. P. Probabilistic Multiple Hazard Resilience Model of an Interdependent Infrastructure System. *Risk Analysis*. 2019.

Li, R. X., Wu, J. G., Li, Y. X. & Cheng, Y. PeriodNet: Noise-Robust Fault Diagnosis Method Under Varying Speed Conditions. *IEEE Transactions on Neural Networks and Learning Systems,* 35**,** 14045-14059. 2024.

Marzocchi, W., Garcia-Aristizabal, A., Gasparini, P., Mastellone, M. L. & Di Ruocco, A. Basic principles of multi-risk assessment: a case study in Italy. *Natural hazards,* 62**,** 551-573. 2012.

Marzocchi, W., Mastellone, M., Di Ruocco, A., Novelli, P. R. E. & Gasparini, P. Principles of multi-risk assessment: Interaction amongst natural and man-induced risks. 2009.

Nguyen, H. T., Wiatr, T., Fernández-Steeger, T. M., Reicherter, K., Rodrigues, D. M. & Azzam, R. Landslide hazard and cascading effects following the extreme rainfall event on Madeira Island (February 2010). *Natural hazards,* 65**,** 635-652. 2013.

Ouyang, M.. A mathematical framework to optimize resilience of interdependent critical infrastructure systems under spatially localized attacks. *European Journal of Operational Research,* 262**,** 1072-1084. 2017

Preston, B. L., Backhaus, S. N., Ewers, M., Phillips, J. A., Dagle, J. E., Silva-Monroy, C., Tarditi, A., Looney, J. & King Jr, T. Resilience of the US electricity system: a multi-hazard perspective. *ORNL, LANL, ANL, SNL, PNNL, and BNL, Tech. Rep*. 2016.

Srivastava, R. & Laurian, L. Natural hazard mitigation in local comprehensive plans: The case of flood, wildfire and drought planning in Arizona. *Disaster Prevention and Management: An International Journal,* 15**,** 461-483. 2006.

Wang, J. W., Gao, Y. & Cheng, Y. On Time-Dependent Critical Platforms and Tracks in Metro Systems. *Transportation Science,* 56**,** 953-971. 2022.

Wei, Y., Cheng, Y. & Liao, H. T. Optimal Resilience-Based Restoration of a System Subject to Recurrent Dependent Hazards. *Reliability Engineering & System Safety,* 247. 2024.

Wei, Y., Li, A., Cheng, Y. & Li, Y. An Optimal Multi-Level Inspection and Maintenance Policy for a Multi-Component System with a Protection Component. *Computers & Industrial Engineering***,** 110898. 2025.

Zhao, S., Wei, Y., Cheng, Y. & Li, Y. A State-Specific Joint Size, Maintenance, and Inventory Policy for a k-out-of-n Load-Sharing System Subject to Self-Announcing Failures. *Reliability Engineering & System Safety***,** 110855. 2025.

Zou, C. Y., Wang, J. W. & Cheng, Y.. Critical Department Analysis for Large-Scale Outpatient Systems. *IEEE Transactions on Computational Social Systems,* 10**,** 3194-3203. 2023a

Zou, C. Y., Wang, J. W. & Cheng, Y. The Impact of the Variability of Patient Flow and Service Time on the Efficiency of Large-Scale Outpatient Systems. *IEEE Transactions on Computational Social Systems,* 10**,** 1230-1240. 2023b.

## Biographies

**Yian Wei** is a PhD student in Department of Data and Systems Engineering, the University of Hong Kong. His research interests include maintenance policy optimization, reliability modeling and resilience modeling.

**Anchi Li** is a PhD student in Department of Data and Systems Engineering, the University of Hong Kong. His research interests include maintenance policy optimization and reliability modeling of complex systems.